Optica Applicata, Vol. XLV, No. 2, 2015
DOI: 10.5277/oa150211

A skew ray tracing approach for error analysis of a light ray path for optical systems with asymmetrical optical axes

TE-TAN LIAO[1], CHIEH KUNG[2*], CHUN-TA CHEN[3]

[1]Department of Mechanical Engineering Far East University,
No. 49, Chung Hua Road, Hsin-Shih, Tainan 744, Taiwan

[2]Department of Industrial Design, Far East University,
No. 49, Chung Hua Road, Hsin-Shih, Tainan 744, Taiwan

[3]Department of Mechatronic Technology, National Taiwan Normal University,
Taipei 106, Taiwan

[*]Corresponding author: julius@cc.feu.edu.tw

This study applies a skew ray tracing approach based on a 4×4 homogeneous coordinate transformation matrix and Snell's law to analyze the errors of a ray light path as it passes through a series of optical elements in an asymmetrical optical system. The proposed error analysis methodology considers two principal sources of a light path error, namely: *i*) the translational errors and the rotational errors which determine the deviation of the light path at each boundary surface, and *ii*) the differential changes induced in the incident point position and unit directional vector of the refracted/reflected ray as a result of differential changes in the position and unit directional vector of the light source. The validity of the proposed methodology is verified by analyzing the effects of optical errors in a corner cube.

Keywords: skew ray tracing, homogeneous coordinate transformation matrix, error analysis.

1. Introduction

Geometric optics not only helps understand the characters of optics and the functions of an optical system, but, more importantly, also provides the knowledge on lenses design. Traditional optic design focuses on the elements of geometric optics. The image quality is to be computed posterior to the design of a lens system in order to assure the design requirements are met. The quality of the image is determined by aberration, energy distribution, and optical transfer function (OTF) [1, 2]. Following the computation of image quality, optimization analysis is conducted. There are two kinds of optimization, namely, local optimization and global optimization. The local optimization is more popular as it only acquires a local minimum. Contrarily, the global optimization requires complicated calculations and consumes time because the global minimum is considered. Theoretically, the optical design including the design of a lens system, analysis of the image quality, and optimization design is based on the assumption that there is no error due to manufacturing process. However, it has been acknowledged that errors including the material, radius of curvature, and flatness of a lens, and tilt and decenter flaws, affect the image quality of a lens system when the lens system is assembled [3–5]. It is thus important to consider the design with the requirements of mechanical and other associated conditions.

There are numerous references on the design and analysis of an optical system [6, 7]. Applications based on relevant theories and principles to the design of instruments of the optical system are available [8, 9]. In light of accompanying new problems and systems that continuously spill out as the era progresses and that mathematical computations might not match the observed image, it is necessary to construct a transferring tool between theories and experiments. The assessment of image quality, either the interpretation of image resolution, image aberration, or OTF, is expected to stand on the theoretical principles so that better and faster measures to designs and analyzes can be achieved.

Evaluating the performance of an optical system during its theoretical design stage requires the ability to determine the paths of the light rays as they undergo reflection and refraction at the boundaries of various optical elements within the system. The light path can be determined using some form of the ray tracing technique, in which the optical laws of reflection and refraction are systematically applied at each boundary encountered by the light ray [10]. The light rays within an optical system can be classified as either axial, meridional or skew [11]. Skew rays, which represent the most general type of a ray, are far more difficult to trace. Nonetheless, without tracing their paths, it is impossible to model optical systems with any degree of reliability or to evaluate their performance. To facilitate the tracing of skew rays, PSANG DAIN LIN [12] reformulated the traditional optical laws of reflection and refraction in terms of revolution geometry, and then conducted a sensitivity analysis based on a skew ray tracing approach to determine the changes in a light ray path as it crossed the boundary between different media.

In the differential ray tracing process, the effects of each optical component are evaluated by differentiating the equations relating the configuration of the rays before and after their transformation at the component surface [13–15]. Such ray tracing approaches enable to assess the sensitivity of an optical system to the design or to manufacturing flaws by correlating the differential changes in the reflected or refracted rays with the differential changes in the incident rays [16, 17]. In their previous work, the authors applied error analysis methods to analyze the errors of a ray's light path as it passes through optical elements with flat [18] and spherical boundary surfaces [19]. The present work extends our previous work to applying the mathematical tools to analyze the errors of a ray's light path as it passes through an axis-symmetrical optical system composed of a series of optical elements with flat and spherical boundary surfaces. The validity of the proposed methodology is verified by analyzing the effects of optical errors in the Petzval lens.

In the analysis presented in this paper, the position vector $P_{ix}\mathbf{i} + P_{iy}\mathbf{j} + P_{iz}\mathbf{k}$ in 3D-space is written in the form of a column matrix ${}^jP_i = [P_{ix}\ P_{iy}\ P_{iz}\ 1]^T$, where the pre-superscript j of the leading symbol ${}^jP_i$ indicates that the vector is referred with respect to the coordinate frame $(xyz)_j$. Given a point ${}^jP_i$, its transformation ${}^kP_i$ is represented by the matrix product ${}^kP_i = {}^kA_j\,{}^jP_i$, where ${}^kA_j$ is a 4×4 matrix defining the position and orientation (referred to hereafter as the configuration) of a frame $(xyz)_j$ with respect to another frame $(xyz)_k$ [20]. The same notation rules are also applied to the unit directional vector ${}^j\ell_i = [\ell_{ix}\ \ell_{iy}\ \ell_{iz}\ 0]^T$. Note that for vectors referred to the world frame $(xyz)_0$, the pre-superscript 0 is omitted for convenience.

2. Skew ray tracing and error analysis at optical boundary surfaces

When performing a geometrical analysis of the performance of an optical system, it is first necessary to define the boundary surfaces within the system in terms of its respective revolution geometries. A ray tracing technique can then be used to determine the paths followed by the skew rays as they undergo successive reflection and refraction operations at various optical surfaces which they encounter as they travel through the system. As shown in Fig. 1, the boundary surface ${}^ir_i$ of an optical element can be obtained by rotating the generating line ${}^ih_i$ in the $x_i y_i$ plane about the y_i axis, *i.e.*,

$$ {}^ir_i = \mathrm{rot}(y_i, \alpha_i)\,{}^ih_i = [R_i\cos(\alpha_i)\cos(\beta_i)\quad R_i\sin(\beta_i)\quad -R_i\sin(\alpha_i)\cos(\beta_i)\quad 1]^T \tag{1} $$

where $\mathrm{rot}(y_i, \alpha_i)$ is the rotation transformation matrix about the y_i axis.

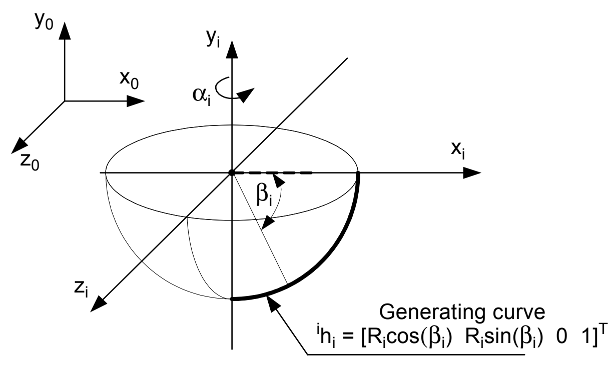

Fig. 1. Medium boundary surface formed by rotating surface geometry.

The unit normal ${}^in_i$ to this boundary surface is given by

$$ {}^in_i = -s_i[\cos(\beta_i)\cos(\alpha_i) \quad \sin(\beta_i) \quad \cos(\beta_i)\sin(\alpha_i) \quad 0]^T \tag{2} $$

where the value of s_i is specified as either +1 or –1 such that the cosine of the incident angle has a positive value, *i.e.*, $\cos(\theta) > 0$.

Note that ${}^ir_i$ and ${}^in_i$ are both expressed with respect to the boundary coordinate frame $(xyz)_j$. The configuration of the world frame $(xyz)_0$ with respect to the boundary coordinate frame is given by

$$ {}^iA_0 = A_{i0} = \begin{bmatrix} I_{ix} & J_{ix} & K_{ix} & t_{ix} \\ I_{iy} & J_{iy} & K_{iy} & t_{iy} \\ I_{iz} & J_{iz} & K_{iz} & t_{iz} \\ 0 & 0 & 0 & 1 \end{bmatrix} \tag{3} $$

where the vectors $[I_{ix} \quad I_{iy} \quad I_{iz} \quad 0]^T$, $[J_{ix} \quad J_{iy} \quad J_{iz} \quad 0]^T$ and $[K_{ix} \quad K_{iy} \quad K_{iz} \quad 0]^T$ describe the orientation of the three unit vectors of frame $(xyz)_0$ with respect to frame $(xyz)_i$. Vector $[t_{ix} \quad t_{iy} \quad t_{iz} \quad 1]^T$ is the position vector of the origin of frame $(xyz)_0$ with respect to frame $(xyz)_i$. The unit normal with respect to the world frame, *i.e.* n_i, can be obtained as

$$ n_i = \begin{bmatrix} n_{ix} \\ n_{iy} \\ n_{iz} \\ 0 \end{bmatrix} = -s_i \begin{bmatrix} I_{ix}\cos(\beta_i)\cos(\alpha_i) + I_{iy}\sin(\beta_i) + I_{iz}\cos(\beta_i)\sin(\alpha_i) \\ J_{ix}\cos(\beta_i)\cos(\alpha_i) + J_{iy}\sin(\beta_i) + J_{iz}\cos(\beta_i)\sin(\alpha_i) \\ K_{ix}\cos(\beta_i)\cos(\alpha_i) + K_{iy}\sin(\beta_i) + K_{iz}\cos(\beta_i)\sin(\alpha_i) \\ 0 \end{bmatrix} \tag{4} $$

Figure 2 shows the general case where a light ray originating at point $P_{i-1} = [P_{i-1x} \quad P_{i-1y} \quad P_{i-1z} \quad 1]^T$ and directed along a unit directional vector $\ell_{i-1} = [\ell_{i-1x}$

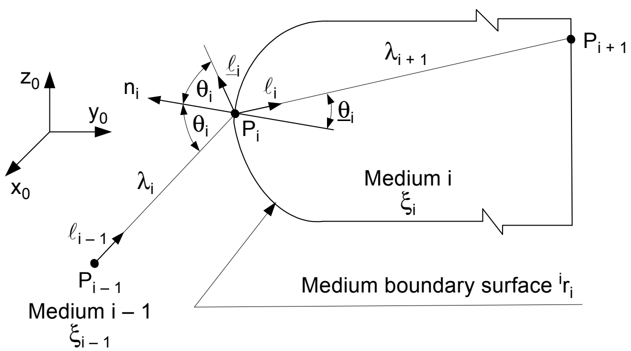

Fig. 2. Skew ray tracing at medium boundary surface ${}^ir_i$.

$\ell_{i-1y}\ \ \ell_{i-1z}\ \ 0]^T$ is reflected/refracted at an optical medium boundary surface ${}^i r_i$. The incident point P_i, refracted ray ℓ_i, and reflected ray $\underline{\ell}_i$ are given by [21]:

$$P_i = \begin{bmatrix} P_{i-1x} + \ell_{i-1x}\lambda_i \\ P_{i-1y} + \ell_{i-1y}\lambda_i \\ P_{i-1z} + \ell_{i-1z}\lambda_i \\ 1 \end{bmatrix}^T \tag{5}$$

$$\ell_i = \begin{bmatrix} \ell_{ix} \\ \ell_{iy} \\ \ell_{iz} \\ 0 \end{bmatrix} = \begin{bmatrix} -n_{ix}\sqrt{1 - N_i^2 + [N_i\cos(\theta_i)]^2} + N_i[\ell_{i-1x} + n_{ix}\cos(\theta_i)] \\ -n_{iy}\sqrt{1 - N_i^2 + [N_i\cos(\theta_i)]^2} + N_i[\ell_{i-1y} + n_{iy}\cos(\theta_i)] \\ -n_{iz}\sqrt{1 - N_i^2 + [N_i\cos(\theta_i)]^2} + N_i[\ell_{i-1z} + n_{iz}\cos(\theta_i)] \\ 0 \end{bmatrix} \tag{6}$$

$$\underline{\ell}_i = \begin{bmatrix} \underline{\ell}_{ix} \\ \underline{\ell}_{iy} \\ \underline{\ell}_{iz} \\ 0 \end{bmatrix} = \begin{bmatrix} \ell_{i-1x} + 2n_{ix}\cos(\theta_i) \\ \ell_{i-1y} + 2n_{iy}\cos(\theta_i) \\ \ell_{i-1z} + 2n_{iz}\cos(\theta_i) \\ 0 \end{bmatrix} \tag{7}$$

where λ_i is the magnitude of vector $P_{i-1}P_i$. The angle of incidence θ_i is given by

$$\cos(\theta_i) = -\ell_{i-1}^T \cdot n_i \tag{8}$$

Note that the term N_i in Eq. (6) is defined as $N_i = \xi_{\text{medium},\, i-1}/\xi_{\text{medium},\, i}$ and represents the ratio of the refractive index of medium $i - 1$ to that of medium i. Following refraction (reflection), the light ray proceeds with point P_i as its new point of origin and ℓ_i as its new unit directional vector.

In optical systems, errors inevitably exist between the designed position and orientation of the optical elements and the actual position and orientation of these elements. In analyzing these errors, the relative positions and orientations of the world frame $(xyz)_0$ with respect to the ideal frame $(xyz)_i$ and the actual frame $(xyz)_a$ can be expressed respectively as

$${}^iA_0 = \begin{bmatrix} I_{ix} & J_{ix} & K_{ix} & t_{ix} \\ I_{iy} & J_{iy} & K_{iy} & t_{iy} \\ I_{iz} & J_{iz} & K_{iz} & t_{iz} \\ 0 & 0 & 0 & 1 \end{bmatrix}, \quad {}^aA_0 = \begin{bmatrix} I_{ax} & J_{ax} & K_{ax} & t_{ax} \\ I_{ay} & J_{ay} & K_{ay} & t_{ay} \\ I_{az} & J_{az} & K_{az} & t_{az} \\ 0 & 0 & 0 & 1 \end{bmatrix} \tag{9}$$

The position and orientation errors of any element within the optical system can be described in terms of three translational errors of the origin of frame $(xyz)_a$, *i.e.*, Δx_i, Δy_i, and Δz_i, and three rotational errors of the three axes of frame $(xyz)_a$ with respect to frame $(xyz)_i$, *i.e.*, $\Delta\omega_{ix}$, $\Delta\omega_{iy}$, and $\Delta\omega_{iz}$ [18]. The overall effect of these six errors can be mathematically expressed using a matrix ${}^iA_a$ of the form

$$ {}^iA_a = \mathrm{trans}(\Delta x_i, \Delta y_i, \Delta z_i)\mathrm{rot}(z, \Delta\omega_{iz})\mathrm{rot}(y, \Delta\omega_{iy})\mathrm{rot}(x, \Delta\omega_{ix}) \tag{10} $$

Since in an optical system, the translational and rotational errors are small, Eq. (10) can be approximated by the first-order Taylor series expansion and rewritten in the form

$$ {}^iA_a = \begin{bmatrix} \bar{I}_{ix} & \bar{J}_{ix} & \bar{K}_{ix} & \bar{t}_{ix} \\ \bar{I}_{iy} & \bar{J}_{iy} & \bar{K}_{iy} & \bar{t}_{iy} \\ \bar{I}_{iz} & \bar{J}_{iz} & \bar{K}_{iz} & \bar{t}_{iz} \\ 0 & 0 & 0 & 1 \end{bmatrix} = \begin{bmatrix} 1 & -\Delta\omega_{iz} & \Delta\omega_{iy} & \Delta x_i \\ \Delta\omega_{iz} & 1 & -\Delta\omega_{ix} & \Delta y_i \\ -\Delta\omega_{iy} & \Delta\omega_{ix} & 1 & \Delta z_i \\ 0 & 0 & 0 & 1 \end{bmatrix} \tag{11} $$

Applying the assumption of ${}^aA_0 = {}^iA_0 + d\,{}^iA_0 = {}^iA_a^{-1}\,{}^iA_0$, it can be shown that

$$ {}^aA_0 = \begin{bmatrix} 1 & \Delta\omega_{iz} & -\Delta\omega_{iy} & -\Delta x_i \\ -\Delta\omega_{iz} & 1 & \Delta\omega_{ix} & -\Delta y_i \\ \Delta\omega_{iy} & -\Delta\omega_{ix} & 1 & -\Delta z_i \\ 0 & 0 & 0 & 1 \end{bmatrix} \begin{bmatrix} I_{ix} & J_{ix} & K_{ix} & t_{ix} \\ I_{iy} & J_{iy} & K_{iy} & t_{iy} \\ I_{iz} & J_{iz} & K_{iz} & t_{iz} \\ 0 & 0 & 0 & 1 \end{bmatrix} \tag{12} $$

Furthermore, differentiating Eqs. (5), (6), and (7), it can be shown that the differential changes in the incident point position ΔP_i, $\Delta\ell_i$, and vector $\Delta\underline{\ell}_i$ are respectively given by:

$$ \Delta P_i = \underline{M}_{P_i} \begin{bmatrix} \Delta P_{i-1} \\ \Delta\ell_{i-1} \end{bmatrix} + S_{P_i}[\Delta e_i] \tag{13} $$

$$ \Delta\ell_i = \underline{M}_{\ell_i} \begin{bmatrix} \Delta P_{i-1} \\ \Delta\ell_{i-1} \end{bmatrix} + S_{\ell_i}[\Delta e_i] \tag{14} $$

$$ \Delta\underline{\ell}_i = \underline{M}_{\underline{\ell}_i} \begin{bmatrix} \Delta P_{i-1} \\ \Delta\ell_{i-1} \end{bmatrix} + S_{\underline{\ell}_i}[\Delta e_i] \tag{15} $$

Combining Eqs. (13), (14), and (15), the differential changes in ΔP_i and the refracted (reflected) ray unit directional vectors $\Delta \ell_i$ ($\Delta \underline{\ell}_i$) can be derived as

$$\begin{bmatrix} \Delta P_i \\ \Delta \ell_i \end{bmatrix} = \underline{M}_i \begin{bmatrix} \Delta P_{i-1} \\ \Delta \ell_{i-1} \end{bmatrix} + S_i [e_i] \tag{16}$$

where $[e_i] = [\Delta x_i \quad \Delta y_i \quad \Delta z_i \quad \Delta \omega_{ix} \quad \Delta \omega_{iy} \quad \Delta \omega_{iz}]^T$. The corresponding light path error induced at the $(n-1)$-th boundary surface can then be determined from

$$\begin{aligned} \begin{bmatrix} \Delta P_{n-1} \\ \Delta \ell_{n-1} \end{bmatrix} &= S_{n-1}[e_{n-1}] + \underline{M}_{n-1} \begin{bmatrix} \Delta P_{n-2} \\ \Delta \ell_{n-2} \end{bmatrix} = \\ &= S_{n-1}[e_{n-1}] + \underline{M}_{n-1} \left\{ S_{n-2}[e_{n-2}] + \underline{M}_{n-2} \begin{bmatrix} \Delta P_{n-3} \\ \Delta \ell_{n-3} \end{bmatrix} \right\} = \\ &= M_{n-1}[e_{n-1}] + M_{n-2}[e_{n-2}] + M_{n-3}[e_{n-3}] + \ldots + M_2[e_2] + M_1[e_1] \end{aligned} \tag{17}$$

In Equation (17), M_i ($i = 1$ to $n-1$) is an error analysis matrix of the i-th boundary surface r_i that can be used to analyze the variation of the exit ray of the optical system. Moreover, M_i combines the ray path errors at the i-th boundary surface (*i.e.*, three translational errors and three rotational errors) with the differential changes induced in the reflected/refracted ray unit directional vector and incident point by differential changes in the light source and unit directional vector of the incident ray.

3. Error analysis of asymmetrical optical system

This section demonstrates the validity of the proposed error analysis methodology using the case of a solid glass corner-cube retroreflector for illustration purposes. A homogeneous solid glass corner-cube has the unique ability to refract and reflect a light ray in directions precisely parallel to that of the incoming ray irrespective of its alignment. The refract and reflect planes for the corner-cube have different optical axis. This particular property of the corner-cubes has been widely applied in the development of safety reflectors and laser tracking measurement systems [22]. In precision measurement applications, the orientation of the incoming ray with respect to the corner-cube must remain constant in order to prevent measurement errors induced by differences in the optical path length [16].

In verifying the proposed error analysis methodology, the boundary surfaces of the solid glass corner-cube are labeled sequentially from 2 to 6 and the coordinate frame $(xyz)_i$ is assigned to the i-th ($i = 2$ to 6) boundary (see Fig. 3). The relative po-

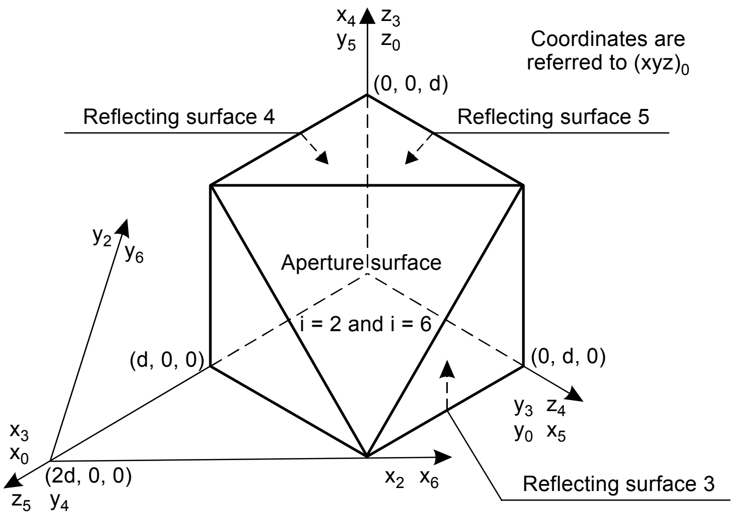

Fig. 3. Coordinate frames used to define flat boundary surface of solid glass corner-cube.

sition and orientation of the world frame $(xyz)_0$ with respect to frame $(xyz)_2$ ($(xyz)_6$) can then be expressed by the following 4×4 homogeneous transformation matrices:

$$^{2}A_0 = {}^{6}A_0 = \begin{bmatrix} -1/\sqrt{2} & 1/\sqrt{2} & 0 & \sqrt{2}\,d \\ -1/\sqrt{6} & -1/\sqrt{6} & 2/\sqrt{6} & 2d/\sqrt{6} \\ 1/\sqrt{3} & 1/\sqrt{3} & 1/\sqrt{3} & -2d/\sqrt{3} \\ 0 & 0 & 0 & 1 \end{bmatrix} \tag{18}$$

where d is the length of the cube edge. The unit directional vector of the incoming ray is given by

$$\ell_1 = \begin{bmatrix} \ell_{1x} \\ \ell_{1y} \\ \ell_{1z} \\ 0 \end{bmatrix} = \frac{1}{\sqrt{6}} \begin{bmatrix} -\sqrt{3}\cos(\beta) - \sin(\beta)\sin(\alpha) + \sqrt{2}\sin(\beta)\cos(\alpha) \\ \sqrt{3}\cos(\beta) - \sin(\beta)\sin(\alpha) + \sqrt{2}\sin(\beta)\cos(\alpha) \\ 2\sin(\beta)\sin(\alpha) + \sqrt{2}\sin(\beta)\cos(\alpha) \\ 0 \end{bmatrix} \tag{19}$$

where β is the polar angle between the x_2 axis and the incoming ray ℓ_1, and α is the polar angle between the normal of the aperture surface and ℓ_1. The impingement point of the incoming ray on the aperture surface (boundary surface 2) is defined as $P_2 = [P_{2x} \;\; P_{2y} \;\; P_{2z} \;\; 1]^T$, where $P_{2x} + P_{2y} + P_{2z} = 2d$ and $0 \le P_{2x} \le d$, $0 \le P_{2y} \le d$, and $0 \le P_{2z} \le d$.

The path of the refracted ray ℓ_2 can then be determined by applying skew ray tracing at the point where the incident ray ℓ_1 passes through the boundary surface 2. The refracted unit directional vector ℓ_2 is therefore given by

$$\ell_2 = \begin{bmatrix} \ell_{2x} \\ \ell_{2y} \\ \ell_{2z} \\ 0 \end{bmatrix} =$$

$$= \frac{-1}{\sqrt{3}} \begin{bmatrix} \sqrt{1 - N_2^2 + N_2^2[\sin(\beta)\cos(\alpha)]^2} + \dfrac{[\sqrt{3}\cos(\beta) + \sin(\beta)\sin(\alpha)]N_2}{\sqrt{2}} \\ \sqrt{1 - N_2^2 + N_2^2[\sin(\beta)\cos(\alpha)]^2} - \dfrac{[\sqrt{3}\cos(\beta) - \sin(\beta)\sin(\alpha)]N_2}{\sqrt{2}} \\ \sqrt{1 - N_2^2 + N_2^2(S\beta C\alpha)^2} - \sqrt{2}\, N_2 S\beta S\alpha \\ 0 \end{bmatrix} \tag{20}$$

where $N_2 = 1/\xi_2$ is the relative refractive index of air, $\xi_1 = 1$, with respect to that of the glass constituting the solid corner cube, *i.e.* ξ_2. Skew ray tracing can then be used at each of the other boundary surfaces to determine the corresponding refracted/reflected rays ℓ_i ($\underline{\ell}_i$) and incident points P_i ($i = 3$ to 6).

In the following discussions, the proposed error analysis methodology is used to determine the differential change in the incident point on the boundary surface 6, ΔP_6, and the corresponding differential change in the unit directional vector of the refracted ray $\Delta\ell_6$ induced by the configuration deviation of the three reflective boundary surfaces of a corner-cube.

A solid glass corner-cube comprises four boundary surfaces, each of which has a unique position and orientation. In discussing ray tracing within a corner-cube, it is necessary to emphasize an unusual feature of the corner-cube which distinguishes it from other optical systems, namely that all the three of its reflective boundary surfaces face the ray ℓ_2 simultaneously, and thus anyone of these surfaces may be the first to encounter the ray. In a previous study [16], the current group considered the case where the internally-reflected ℓ_2 light ray followed paths ($3 \to 4 \to 5$) or ($5 \to 3 \to 4$), for example. By contrast, the following analysis assumes a path sequence of $2 \to 3 \to \to 4 \to 5 \to 6$. From Eq. (17), the error of an exit ray, *e.g.* $[\Delta P_6 \ \ \Delta\ell_6]^T$, can be analyzed in terms of the deviations of the light ray in each of the six degrees of freedom with respect to the coordinate frame on the i-th ($i = 2$ to 6) boundary surface, *i.e.*

$$\begin{bmatrix} \Delta P_6 \\ \Delta \ell_6 \end{bmatrix} = \underline{M}_6[e_6] + \underline{\underline{M}}_6 \begin{bmatrix} \Delta P_5 \\ \Delta \ell_5 \end{bmatrix} = \underline{M}_6[e_6] + \underline{\underline{M}}_6 \left\{ \underline{M}_5[e_5] + \underline{\underline{M}}_5 \begin{bmatrix} \Delta P_4 \\ \Delta \ell_4 \end{bmatrix} \right\} =$$

$$= \underline{M}_6[e_6] + \underline{\underline{M}}_6 \underline{M}_5[e_5] + \underline{\underline{M}}_6 \underline{\underline{M}}_5 \begin{bmatrix} \Delta P_{n-3} \\ \Delta \ell_{n-3} \end{bmatrix} =$$

$$= M_6[e_6] + M_5[e_5] + M_4[e_4] + M_3[e_3] + M_2[e_2] + M_1[e_1] \tag{21}$$

The error analysis matrix M_i has the form

$$M_i = \begin{bmatrix} 0 & 0 & \frac{\partial P_{ix}}{\partial z_i} & \frac{\partial P_{ix}}{\partial \omega_{ix}} & \frac{\partial P_{ix}}{\partial \omega_{iy}} & 0 \\ 0 & 0 & \frac{\partial P_{iy}}{\partial z_i} & \frac{\partial P_{iy}}{\partial \omega_{ix}} & \frac{\partial P_{iy}}{\partial \omega_{iy}} & 0 \\ 0 & 0 & \frac{\partial P_{iz}}{\partial z_i} & \frac{\partial P_{iz}}{\partial \omega_{ix}} & \frac{\partial P_{iz}}{\partial \omega_{iy}} & 0 \\ 0 & 0 & 0 & \frac{\partial \ell_{ix}}{\partial \omega_{ix}} & \frac{\partial \ell_{ix}}{\partial \omega_{iy}} & 0 \\ 0 & 0 & 0 & \frac{\partial \ell_{iy}}{\partial \omega_{ix}} & \frac{\partial \ell_{iy}}{\partial \omega_{iy}} & 0 \\ 0 & 0 & 0 & \frac{\partial \ell_{iz}}{\partial \omega_{ix}} & \frac{\partial \ell_{iz}}{\partial \omega_{iy}} & 0 \end{bmatrix} \begin{bmatrix} \Delta x_i \\ \Delta y_i \\ \Delta z_i \\ \Delta \omega_{ix} \\ \Delta \omega_{iy} \\ \Delta \omega_{iz} \end{bmatrix}, \quad i = 3 \text{ to } 5 \tag{22}$$

The following discussions analyze the differential changes in the position and orientation of an exit ray $[\Delta P_6 \quad \Delta \ell_6]^T$ in terms of the differential changes in the translational errors and rotational errors, respectively, at each of the three reflective boundary surfaces of the corner-cube. In general, the translational errors Δx_i and Δy_i and the rotational error $\Delta \omega_{iz}$ do not influence the position of the exit ray, and hence the variations $\partial P_6/\partial x_i$, $\partial P_6/\partial y_i$, and $\partial P_6/\partial \omega_{iz}$ ($i = 3$ to 5) are equal to zero. Figure 4 illustrates the variation of $\partial P_6/\partial z_i$ ($\partial P_6/\partial z_i = (\partial P_{6x}/\partial z_i + \partial P_{6y}/\partial z_i + \partial P_{6z}/\partial z_i)^{1/2}$, $i = 3$ to 5) with changes in the polar angle of the incoming ray α for constant $P_{2x} = 0.8d$, $P_{2y} = 0.75d$, $P_{2z} = 0.45d$, $\xi_2 = 1.6$ and different $\beta = 90°$, $\beta = 95°$. The results show that variations in the translation error Δz_i have a comparatively pronounced effect on the variation of the incident point position on the boundary surface 6, P_6. Figure 4 shows that when $\beta = 90°$, reflect planes 4 and 5 have the same effect on the deviation of exit point P_6.

Figure 5 demonstrates the effect of the rotational error $\Delta \omega_{ix}$ on the differential change in $\partial P_6/\partial \omega_{ix}$ ($\partial P_6/\partial \omega_{ix} = (\partial P_{6x}/\partial \omega_{ix} + \partial P_{6y}/\partial \omega_{ix} + \partial P_{6z}/\partial \omega_{ix})^{1/2}$, $i = 3$ to 5) for

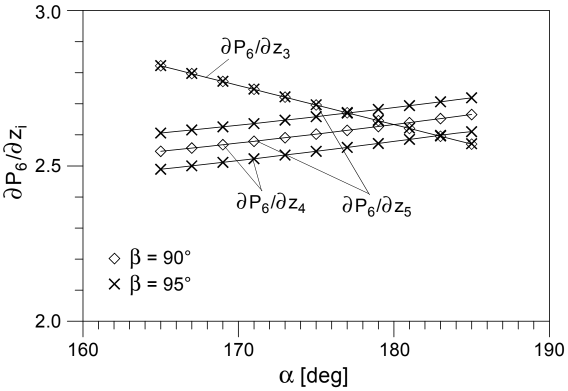

Fig. 4. Variation of $\partial P_6/\partial z_i$ (i = 3, 4, 5) with α on three reflecting surfaces of corner-cube.

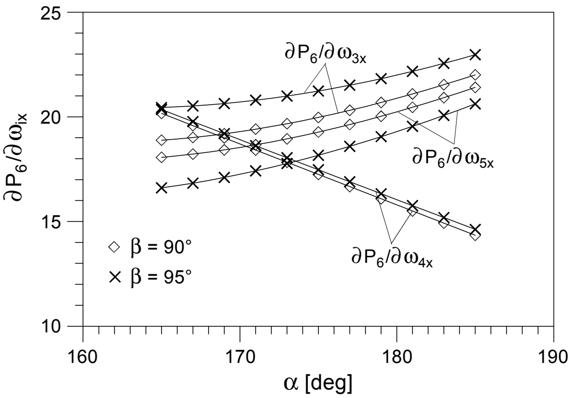

Fig. 5. Variation of $\partial P_6/\partial \omega_{ix}$ (i = 3, 4, 5) with α on three reflecting surfaces of corner-cube.

different values of the polar angle α with $\beta = 90°$, $\beta = 95°$. Compared to the translation error Δz_i it is apparent that changes in the rotational error have a more marked effect on the changes induced in the position of the ray exiting the corner-cube from the boundary surface 6.

The normal directions of the three reflective surfaces are independent of the translational errors and rotational error of the z-axis at each surface, and hence the direction of the reflected ray is unchanged during the reflection process. As a result, the variations of $\partial \ell_6/\partial x_i$, $\partial \ell_6/\partial y_i$, $\partial \ell_6/\partial z_i$ and $\partial \ell_6/\partial \omega_{iz}$ (i = 3 to 5) are equal to zero. Figure 6 shows the effects of the rotational error $\Delta \omega_{ix}$ at each of the three reflective surfaces on the differential change of the unit directional vector at the boundary surface 6, *i.e.* $\partial \ell_6/\partial \omega_{ix}$ ($\partial \ell_6/\partial \omega_{ix} = (\partial \ell_{6x}/\partial \omega_{ix} + \partial \ell_{6y}/\partial \omega_{ix} + \partial \ell_{6z}/\partial \omega_{ix})^{1/2}$, i = 3 to 5) for different values of the polar angle α, $\beta = 90°$, $\beta = 95°$.

In general, Figs. 4 to 6 demonstrate that deviations of the incident position and orientation of the light ray at the reflective boundary surfaces of a corner-cube lead to deviations in the position and orientation of the light ray at the exit surface. In practical

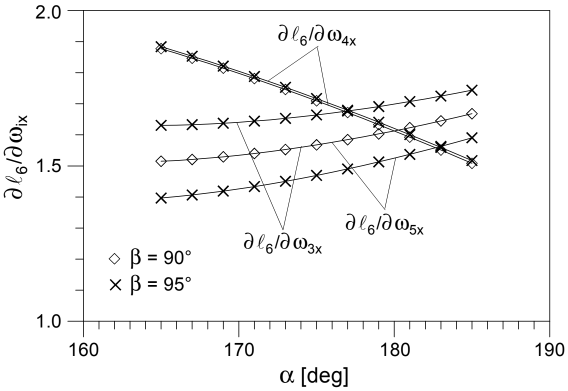

Fig. 6. Variation of $\partial\ell_6/\partial\omega_{ix}$ (i = 3, 4, 5) with α on three reflecting surfaces of corner-cube.

terms, the present results indicate that in precision measurement applications, a constant orientation must be maintained between the incoming ray and the corner-tube, and the three reflective boundary surfaces must be arranged mutually perpendicular to one another in order to prevent measurement errors induced by differences in the optical path length and differential changes in the position and orientation of the exit ray, respectively.

4. Conclusion

The performance of an optical system is limited not only by image aberrations induced by the individual components within the system, but also by assembly errors introduced during its construction. The validity of the proposed methodology has been demonstrated by analyzing the asymmetrical corner-cube retroreflector. The methodology considers two fundamental sources of error, namely *i*) the translational errors (Δx_i, Δy_i, and Δz_i) and rotational errors ($\Delta\omega_{ix}$, $\Delta\omega_{iy}$, and $\Delta\omega_{iz}$) which govern the deviation of the light path at each boundary surface; and *ii*) the differential changes in the incident point and unit directional vector of the refracted/reflected ray as a result of differential changes in the position and unit directional vector of the light source. When the incident light unit direction vector is different at different angles α and β for a corner cube, the effect of the translation and rotation error for the optical component boundary on the deviation of the position and direction for an exit light is different. The results in this paper show that manufacturing error and assembling error will affect the performance of optical systems, and reduce the precision of optical systems.

Acknowledgments – The financial support provided to this study by the National Science Council of Taiwan under grant NSC102-2221-E-269-007 is gratefully acknowledged.

References

[1] FISHER R.E., *Optical Systems Design*, McGraw Hill, New York, 2000.
[2] KINGSLAKE R., *Optical System Design*, Academic Press, New York, 1983.

[3] KIM K., EMAN K.F., WU S.M., *Analysis alignment errors in a laser-based in-process cylindricity measurement system*, Transaction of the ASME Journal of Engineering for Industry **109**(4), 1987, pp. 321–329.

[4] HOPKINS H.H., TIZIANI H.J., *A theoretical and experimental study of lens centering errors and their influence on optical image quality*, British Journal of Applied Physics **17**(1), 1966, pp. 33–54.

[5] LAIKIN M., *Lens Design*, Marcel Dekker, New York, 1995.

[6] SMITH W.J., *Modern Lens Design*, Genesse Optics Software, McGraw-Hill, Rochester, New York, 1992.

[7] HOWARD J.M., *Optical design using computer graphics*, Applied Optics **40**(19), 2001, pp. 3225–3231.

[8] CHUNYU ZHAO, BURGE J.H., *Application of the pupil astigmatism criteria in optical design*, Applied Optics **41**(34), 2002, pp. 7288–7293.

[9] SABATKE E.E., BURGE J.H., HINZ P., *Optical design of interferometric telescopes with wide fields of view*, Applied Optics **45**(31), 2006, pp. 8026–8035.

[10] HERZBERGER M., *Modern Geometrical Optics*, Interscience Publishers, New York, 1958.

[11] HECHT E., *Optics*, Addison-Wesley, New York, 1998.

[12] PSANG DAIN LIN, *Analysis and modeling of optical element and systems*, Transaction of the ASME Journal of Engineering for Industry **116**(1), 1994, pp. 101–107.

[13] FORBES G.W., *Accuracy doubling in the determination of the final ray configurations*, Journal of the Optical Society of America A **6**(11), 1989, pp. 1776–1783.

[14] STONE B.D., *Determination of initial ray configurations for asymmetric systems*, Journal of the Optical Society of America A **14**(12), 1997, pp. 3415–3429.

[15] WEI WU, PSANG DAIN LIN, *Numerical approach for computing the Jacobian matrix between boundary variable vector and system variable vector for optical systems containing prisms*, Journal of the Optical Society of America A **28**(5), 2011, pp. 747–758.

[16] TE-TAN LIAO, PSANG DAIN LIN, *Analysis of optical elements with flat boundary surfaces*, Applied Optics **42**(7), 2003, pp. 1191–1202.

[17] CHUANG-YU TSAI, PSANG DAIN LIN, *Prism design based on changes in image orientation*, Applied Optics **45**(17), 2006, pp. 3951–3959.

[18] TE-TAN LIAO, *A skew ray tracing-based approach to the error analysis of optical elements with flat boundary surfaces*, Optik – International Journal for Light and Electron Optics **119**(15), 2008, pp. 713–722.

[19] TE-TAN LIAO, CHUN-TA CHEN, *A skew ray tracing approach for the error analysis of optical elements with spherical boundary surfaces*, Journal of Modern Optics **55**(12), 2008, pp. 1981–2002.

[20] PAUL R.P., *Robot Manipulators: Mathematics, Programming and Control*, MIT Press, Cambridge, MA, 1981.

[21] PSANG DAIN LIN, TE-TAN LIAO, *A new model of binocular stereo coordinate measurement system based on skew ray tracing*, Journal of Dynamic Systems, Measurement, and Control **126**(1), 2004, pp. 102–114.

[22] *Leica Smart 310 Laser Tracker Owner's Manual*, Leica Geosystems AG, Heerbrugg, Switzerland, 1987.

Received January 6, 2015
in revised form January 26, 2015